Chinese Journal of Chemical Engineering

New process development and process evaluation for capturing CO_2 in flue gas from power plants using ionic liquid [emim][Tf_2N]

Lan Li[1,2,3], Xiaoting Huang [1,2,3], Quanda Jiang[4], Luyue Xia[1], Jiawei Wang[5] and Ning Ai [1,2,3*]

[1] College of Chemical Engineering, Zhejiang University of Technology, Hangzhou 310014, Zhejiang, China
[2] Zhejiang Province Key Laboratory of Biomass Fuel, Hangzhou 310014, Zhejiang, China
[3] Biodiesel Laboratory of China Petroleum and Chemical Industry Federation, Hangzhou 310014, Zhejiang, China
[4] Zhe Jiang Supcon Software Co.,LTD,Hangzhou 310014, Zhejiang, China
[5] School of Engineering & Applied Science, Aston University, Birmingham B4 7ET, W Midlands, England
*Corresponding author: aining@tsinghua.org.cn

Abstract

Using the ionic liquid [emim][Tf_2N] as a physical solvent, it was found by aspen plus simulation that it was possible to attempt to capture CO_2 from the flue gas discharged from the coal-fired unit of the power plant. Using the combination of model calculation and experimental determination, the density, isostatic heat capacity, viscosity, vapor pressure, thermal conductivity, surface tension and solubility of [emim][Tf_2N] were obtained. Based on the NRTL model, the Henry coefficient and NRTL binary interaction parameters of CO_2 dissolved in [emim][Tf_2N] were obtained by correlating [emim][Tf_2N] with the gas-liquid equilibrium data of CO_2. Firstly, the calculated relevant data is imported into Aspen plus, and the whole process model of the ionic liquid absorption process is established. Then the absorption process is optimized according to the temperature distribution in the absorption tower to obtain a new absorption process. Finally, the density, constant pressure heat capacity, surface tension, thermal conductivity, viscosity of [emim][Tf_2N] were changed to investigate the effect of ionic liquid properties on process energy consumption, solvent circulation and heat exchanger design.The results showed that based on the composition of the inlet gas stream to the absorbers, CO_2 with a capture rate of 90% and a mass purity higher than 99.5% was captured; These results indicate that the [emim][Tf_2N] could be used as a physical solvent for CO_2 capture from coal-fired units.In addition,The results will provide a theoretical basis for the design of new ionic liquids for CO_2 capture.

Keywords

Ionic liquids;CO_2 capture; Aspen plus process simulation;New green physical solvents;Flue gas

1.Introduction

In recent years, global warming caused by massive emissions of greenhouse gases has become increasingly serious. In order to curb this trend, people have done a lot of work around CO_2 emission reduction. Carbon Capture and Storage (CCS) is considered to be the

most economical and viable way to reduce CO_2 emissions in the short term [1]. The chemical absorption method using an alcohol amine solution as an absorbent is currently the most widely used CO_2 capture means [2].

Shupanxiang Chen et al [3]. applied a stopped-flow apparatus to study the kinetics of the absorption of CO_2 in non-aqueous blended DMEA-MEA and DEEA-MEA solutions and demonstrated that there are interactions between the tertiary amine and the primary amine in the non-aqueous blended amine system that positively promote the kinetics. Thereby it accelerated the total reaction rate of the mixed amines to absorb CO_2.

However, the alcohol amine method has technical difficulties such as solvent degradation, volatilization, strong corrosiveness to equipment and high energy consumption for regeneration. Therefore, there is an urgent need to find a greener solvent to replace the traditional alcohol amine solution. In recent years, related research has shown that ionic liquids have good solubility absorption capacity for CO_2 and ionic liquids (Ionic Liquids, referred to as ILs) are considered as possible substitutes for traditional volatile organic solvents [4].

Ionic liquids are also called Room temperature ionic liquids (RTILs), which are organic molten salts composed of organic cations and inorganic or organic anions at room temperature(298.15k) or near room temperature [5]. Ionic liquids have received extensive attention due to their extremely low saturated vapor pressure, almost non-volatile and good thermochemical stability [6-11]. They are regarded as "new green solvents" after supercritical carbon dioxide [4]. Ionic liquids are designed to be designed to develop new ionic liquids with high CO_2 solubility, enabling them to be used to capture CO_2 from industrial waste gases and the atmosphere. Thereby solving the problems of corrosion and complicated post-treatment of high-volatility traditional organic solvents in the existing CO_2 absorption process [12,13].

Since the first experimental study by Blanchard et [14,15]. In 1999, it has been found that CO_2 has a high solubility in ionic liquids. The research of ionic liquids in the field of carbon capture is still in a feverish state, and ionic liquids with better performance are continuously discovered and synthesized.

Shiflett et al[16]. used the RK equation of state to correlate the dissolved phase equilibrium data of CO_2 in [bmim][Ac] to simulate the ionic liquids absorption CO_2 process. The energy consumption is minimized by optimizing the operating pressure of the absorber and the amount of absorbent, and the energy consumption of the regeneration process is reduced by 16% compared to conventional monoethanolamine absorbents.

Ma et al [17]. used Aspen plus to calculate the physical property data of [bmim][BF_4] and [bmim][PF_4], and selected the ENRTL model to calculate thermodynamic data such as density, constant pressure heat capacity and saturated vapor pressure, using NRTL model and The RK model calculates the gas-liquid equilibrium (VLE) data of the system, and the results are consistent with the experimental data. The loss of 1 t CO_2 per ionic liquids [bmim][BF_4] and [bmim][PF_4] was 0.229 g and 0.391 g, respectively, while the conventional solvent MEA had a unit loss of 178 g/t CO_2. The capture energy consumption was reduced by 26.7% and 24.8%, respectively, compared to the MEA process.

Huang et al [18]. used Aspen plus as a simulation platform to absorb three kinds of compound solutions [bmim][BF_4]-MEA, [bmim][DCA]-MEA, [bpy][BF_4]-MEA and traditional MEA solution. The CO_2 process was simulated to compare the energy consumption and cost of each process. The results show that the [bpy] [BF_4]-MEA compound solution saves 15% energy consumption and 11% capture compared to conventional MEA solutions. The process of using the [bpy][BF_4]-MEA compound solution as an absorbent is improved, and the cooling tower of the absorption tower is cooled and the desorbing tower depleted steam recompression device is increased, and the process energy is improved

compared to the process using the conventional MEA solvent. Consumption and capture costs were reduced by 31% and 13.5%, respectively.

The above-mentioned literature reports mainly carry out process simulations around the prepared ionic liquids, failing to combine the capture process to guide the synthesis and development of ionic liquids. Ionic liquids have certain advantages compared with traditional solvents, but the process research and simulation research of ionic liquids trapping CO_2 are lagging behind. Further work is needed to realize that ionic liquids really replace traditional solvents. The purpose of this paper is to design a decarburization process for the flue gas emitted by Shen hua Guo hua jie 600 MW subcritical coal-fired unit [19-22] with ionic liquid [emim][Tf_2N] as the absorbent, and use Aspen plus. The software simulates, optimizes and evaluates the process, and selects the most suitable thermal conductivity, constant pressure heat capacity, vapor pressure, viscosity, density, surface tension of the ionic liquids to absorb CO_2 according to the simulation results, and the properties of the ionic liquids itself. And the impact of equipment selection, the result shows that the ionic liquid based capture system is a feasible alternative to the traditional solvent.

2. Properties of [emim][Tf_2N]

The physical properties of the ionic liquids involved in the process simulation also include thermal conductivity, constant pressure heat capacity, vapor pressure, viscosity, density, surface tension, binary exchange parameters of ionic liquids and gases. The experimental data of ionic liquids were obtained by consulting literature and experiments, and the above parameters were fitted by least squares method. The objective function of the optimization model is the minimum variance of the corresponding parameters. The calculation formula is as follows:

$$OF = \sum_{i=1}^{N_P} (X_i^{cal} - X_i^{exp})^2 \qquad (1)$$

The accuracy of the fitted regression is judged by the mean absolute relative deviation (AARD). The specific formula is as follows:

$$AARD(\%) = 100 \times \frac{\sum_{i=1}^{N_P} \left| \frac{X_i^{cal}}{X_i^{exp}} - 1.0 \right|}{N_P} \qquad (2)$$

In Eqs. (1), (2) X represents the data points of the above temperature-related properties, cal and exp represent calculated and experimental values, i is the data point number, and N_P is the total number of data points.

2.1 Density

Different density values for [emim][Tf_2N] are available in the literature reported by Schilderman et al.[23]at various temperatures and 0.1 MPa. These values were correlated using the Rackett equation In the Aspen plus .

2.2 Heat capacity

Using a scanning calorimeter for measuring the heat capacity of [emim][Tf_2N] at a constant pressure from 343.15 K to 463.15 K, was reported by Ferreira et al [24].

2.3Viscosity

Liu Xiangyang et al [7] measured the viscosity of [emim][Tf_2N] using a Brookfield DV-II+Pro viscometer. The viscosities were available using a Vogel-Fulchner-Tammann liquid viscosity correlation as functions of temperature in the range of 273.15 K to 363.15 K.

2.4 Vapor pressure

The vapor pressure of the ionic liquids is so low that difficult to measure at normal

temperature and pressure. Heym et al [25] measured the vapor pressure of [emim][Tf_2N] at 538.13 K-723.13 K by thermogravimetric analysis. The relationship between vapor pressure and temperature was obtained by fitting the Antoine equation. The calculated evaporation enthalpy was 120kJ•mol^{-1}.

2.5 Thermal conductivity

The Temperature-dependent method for calculating The thermal conductivity of [emim][Tf_2N] at 273.15K-353.15 K was Adopted by Fröba et al [26].

2.6 Surface tension

The vast majority of ionic liquids have much greater surface tension than air in conventional organic solvents.The surface tension of ionic liquids was measured by Tariq et al.[27] at 313 K -532 K.

2.7Gases solubilities

The methods for determining the solubility of a gas in an ionic liquids are mainly quartz crystal microbalance method [28], gravity balance method[29], weighing method[30], bubble point method[31], gas chromatography method [32], and constant volume method[33]. In this chapter, the constant volume method is used to determine the solubility of CO_2 in ionic liquids. The basic principle is to determine the gas change before and after absorption by measuring the pressure of the gas before and after absorption in a constant volume container. The two-phase composition can be obtained according to the material balance. Thereby, The method of obtaining the solubility of the gas in the ionic liquids effectively solves the problem that the gas-liquid two-phase sampling will destroy the formed gas-liquid equilibrium.

The schematic diagram of the gas-liquid equilibrium experimental device based on the constant volume method is shown in **Fig.1**.

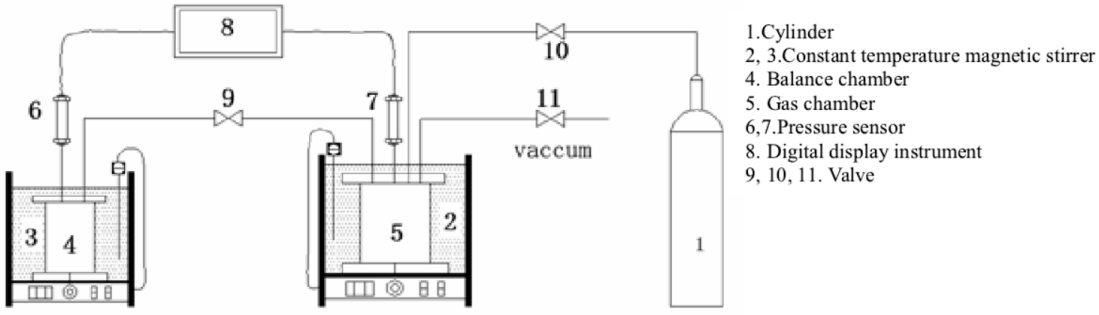

Fig.1. Schematic diagram of the experimental apparatus.

In Fig.1 the core devices are the balance chamber (4) and the gas chamber (5). The balance chamber volume is 370.99 cm^3, and the gas buffer chamber (5) has a volume of 141.61 cm^3. The temperature of the gas buffer chamber and the balance chamber are controlled by two constant temperature water baths (2, 3) with an accuracy of ±0.05 K. The pressure of the gas buffer chamber and the balance chamber is measured by a pressure sensor with a sensor range of 0-0.9MPa and an accuracy of 0.1%. The temperature and pressure of the gas buffer chamber and the balance chamber are respectively displayed on the digital display (8).

3. Modeling of gas solubility using the NRTL-RK EOS

The process simulation performed on Aspen plus requires the selection of a physical property database already in the software. In general, the molecular weight of the ionic liquids is relatively large, and its intermolecular force is similar to that of a highly polar organic solvent. The ionic liquids system can be calculated by a thermodynamic model of a strong polar solution such as the activity coefficient method [35]. The commonly used

models of activity coefficients are WILSON, NRTL, UNIQUAC and UNIFAC. Due to the high pressure process in the process, the gas phase cannot be treated as an ideal gas. Therefore, the physical property method can select the NRTL-RK equation. The specific calculation formula is as follows:

$$\gamma_{\mathrm{i}}^{*}=\frac{\gamma_{\mathrm{i}}}{\gamma_{i}^{\infty}} \quad (3)$$

$$\lim_{x_i\to 0}\gamma_{\mathrm{i}}^{*}=1 \quad (4)$$

$$\varphi_{\mathrm{i}}^{\mathrm{V}} y_{\mathrm{i}} p=x_{\mathrm{i}}\gamma_{\mathrm{i}}^{*} H_{\mathrm{iA}} \quad (5)$$

The Henry coefficient calculation formula in the process simulation is as follows:

$$H_{\mathrm{iA}}=\lim_{x_i\to 0}\frac{f_{\mathrm{i}}}{x_{\mathrm{i}}}=\lim_{x_i\to 0}\frac{\varphi_{\mathrm{i}}^{\mathrm{V}} y_{\mathrm{i}} p}{x_i} \quad (6)$$

$$\ln H_{\mathrm{iA}}=a_{\mathrm{iA}}+\frac{b_{\mathrm{iA}}}{T}+c_{\mathrm{iA}}\ln T+d_{\mathrm{iA}}T \quad (7)$$

Where a_{iA}、b_{iA}、c_{iA}、d_{iA} are Henry's coefficient model equation parameters□□

$$\ln\varphi^{\mathrm{V}}=Z-1-\ln(Z-\frac{bp}{RT})-(\frac{a/R^2T^{2.5}}{b/RT})\ln(1+\frac{bp}{ZRT}) \quad (8)$$

$$Z=\frac{pV}{RT} \quad (9)$$

The fugacity coefficient of the gas is calculated by the RK equation. The specific calculation formula is as follows:

$$p=\frac{RT}{V-b}-\frac{a}{T^{0.5}V(V+b)} \quad (10)$$

$$a=0.42748\frac{R^2T_{\mathrm{c}}^{2.5}}{p_{\mathrm{c}}} \quad (11)$$

$$b=0.08664\frac{RT_{\mathrm{c}}}{p_{\mathrm{c}}} \quad (12)$$

The specific content of the NRTL model equation is as follows:

$$\ln\gamma_{\mathrm{i}}=\frac{\sum_{\mathrm{j=1}}^{\delta}x_{\mathrm{j}}\tau_{\mathrm{ji}}G_{\mathrm{ji}}}{\sum_{\mathrm{k=1}}^{\delta}x_{\mathrm{k}}G_{\mathrm{ki}}}+\sum_{\mathrm{j=1}}^{\delta}\left[\frac{x_{\mathrm{j}}G_{\mathrm{ij}}}{\sum_{\mathrm{k=1}}^{\delta}x_{\mathrm{k}}G_{\mathrm{kj}}}\left[\tau_{\mathrm{ij}}-\frac{\sum_{\mathrm{m=1}}^{\delta}x_{\mathrm{m}}\tau_{\mathrm{mj}}G_{\mathrm{mj}}}{\sum_{\mathrm{k=1}}^{\delta}x_{\mathrm{k}}G_{\mathrm{kj}}}\right]\right] \quad (13)$$

$$G_{\mathrm{ij}}=\exp(-\alpha_{\mathrm{ij}}\tau_{\mathrm{ij}}) \quad (14)$$

$$\tau_{\mathrm{ij}}=a_{\mathrm{ij}}+b_{\mathrm{ij}} \quad (15)$$

$$\alpha_{\mathrm{ij}}=\alpha_{\mathrm{ji}}=0.3 \quad (16)$$

Where $a_{\mathrm{ij}}, b_{\mathrm{ij}}$ are the NRTL model parameters.

In order to perform the calculations, the critical properties and binary interaction parameters between the gases and ILs are required.

3.1 Critical properties .

The critical parameters of [emim][Tf_2N] were evaluated using themodified group contributions estimation method as reported by Valderrama et al [35] and Robles et al [34]. The specific equations involved in this method are as follows:

$$T_b = 198.2 + \sum n\Delta T_b \quad (17)$$

$$T_c = \frac{T_b}{[0.5703 + 1.0121\sum n\Delta T_c - (\sum n\Delta T_c)^2]} \quad (18)$$

$$P_c = \frac{M}{[0.2573 + \sum n\Delta P_c]^2} \quad (19)$$

$$V_c = 6.75 + \sum n\Delta V_c \quad (20)$$

$$Z_c = \frac{P_c V_c}{RT_c} \quad (21)$$

where n is the number of times that a group appears in the molecule and ΔT_b, ΔT_c, and ΔV_c correspond to the contribution to the critical properties. The values of these parameters were obtained from Valderrama et al.In addition, Eqs. (22) known as Rudkin's equation, was used to determine the acentric factor at the normal boiling temperature:

$$\omega = \frac{(T_b - 43)(T_c - 43)}{(T_c - T_b)(0.7T_c - 43)} \log\left[\frac{P_c}{P_b}\right] - \frac{(T_c - 43)}{(T_c - T_b)} \log\left[\frac{P_c}{P_b}\right] + \log\left[\frac{P_c}{P_b}\right] - 1 \quad (22)$$

The critical parameters of the ionic liquids were calculated using the modified Lydersen-Joback-Reid group contribution method. **Table1** shows the critical parameters of theionic liquid.

Table 1. Calculated critical parameter of ionic liquids.

Physical parameters	M/g.mol^{-1}	T_b/K	T_c/K	P_c/Mpa	V_c/cm^3.mol^{-1}	Z_c	ω
[emim][Tf_2N]	391.321	816.68	1249.31	3.2653	875.91	0.2715	0.2157

3.2. Binary interaction parameters

For the phase equilibrium data of the binary system CO_2-[emim][Tf_2N], the solubility of the ionic liquids under low pressure conditions was measured by a gas-liquid phase equilibrium device. Solubility data at medium and high pressures were directly reported using data reported by Astrid et al [23] and Takashiet al[36]. Parametric regression is performed on the above model equations (Eqs. (3)- (16)) using the least squares method. The result is shown in **Table 2,Table 3.**

Table 2. Parameters of temperature-dependent Henry Constants.

Component i	Component A	a_{iA}	b_{iA}	c_{iA}	d_{iA}	e_{iA}
CO_2	[emim][Tf_2N]	82.14872	0.0051699	-12.95448	0.0051714	-874200

Table 3 NRTL binary parameters of CO_2 with [emim][Tf_2N].

Component i	Component j	a_{ij}	a_{ji}	b_{ij}	b_{ji}
CO_2	[emim][Tf_2N]	1.26676	-4.902826	-671.2823	1685.225

4.Experimental results

4.1 Ionic liquids' properties.

Ionic Liquids' Properties. The properties of Ionic Liquids are presented in **Fig. 2- 7.**in the Supporting Information and were modeled using the correlations presented in **Table 4**. It can be known from AARD that the fitting results of each parameter are better.

Table 4. Correlations and parameters developed for various properties of the [emim][Tf_2N].

Property	Units	Correlation	Parameters	Data	AARD(%)

Density	g.cm^{-3}	$\rho_i = \frac{M_i p_{ci}}{RT_{ci} Z_i^{*,RA\left(1+(1-T_r)^{2/7}\right)}}$	$Z_i^{*,RA}$	0.2716273	0.0205
Heat capacity	J·mol^{-1}·K^{-1}	$C_{pi} = C_{1i}^{'} + C_{2i}^{'} T + C_{3i}^{'} T^2$	$C_{1i}^{'}$ $C_{2i}^{'}$ $C_{3i}^{'}$	329.3281 0.84934 -0.0007677	0.063116
Viscosity	MPa·s	$\ln \eta_i = A_i + \frac{B_i}{T} + C_i \ln(T)$	A_i B_i C_i	-138.1042 9054.914 19.52435	0.3117
Vapor pressure	MPa	$\ln p_i^s = C_{1i} + \frac{C_{2i}}{T}$	C_{1i} C_{2i}	28.37476 -15130	0. 3359767
Thermal conductivity	W·m^{-1}·K^{-1}	$\lambda_i = C_{1i}^{''} + C_{2i}^{''} T + C_{3i}^{''} T^2$	$C_{1i}^{''}$ $C_{2i}^{''}$ $C_{3i}^{''}$	0.1339236 -0.0000613 4.957×10^{-8}	0.392
Surface tension	mN·m^{-1}	$\sigma_i = C_{1i}^{'''}(1-\frac{T}{T_{ci}})^{(C_{2i}^{'''}+C_{3i}^{'''}T_{ri}+C_{4i}^{'''}T_{ri}^{2}+C_{5i}^{'''}T_{ri}^{3})}$	$C_{1i}^{'''}$ $C_{2i}^{'''}$ $C_{3i}^{'''}$ $C_{4i}^{'''}$ $C_{5i}^{'''}$	103.2335 15.6131 -92.9548 234.0923 -204.9143	1.0600

The comparison between the experimental values of the ionic liquid [emim][Tf_2N] density and the calculated values in the range of 273.15 K to 363.15 K is shown in **Fig.2** and the agreement shows that the degree of coincidence is good.

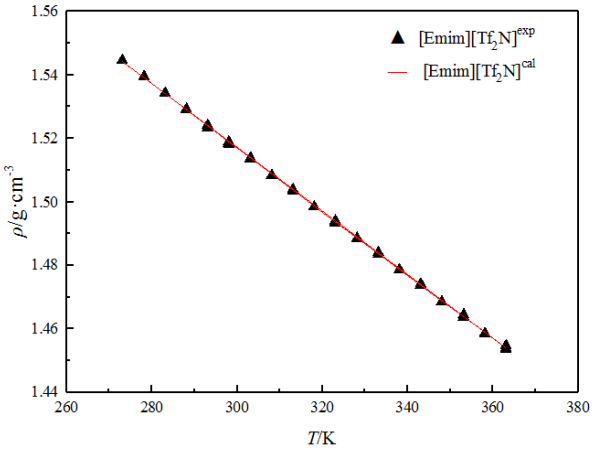

Fig.2. Density fitting effect of [emim][Tf_2N].

Fig.3 shows the comparison between the experimental values of the isobaric heat capacity of the [emim][Tf_2N] and the fitted calculations. The data is in the range of 343.15 K to 463.15 K.

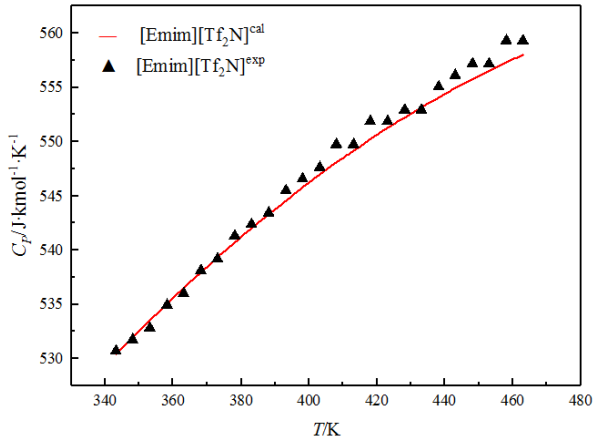

Fig. 3. Isometric heat capacity fitting effect of [emim][Tf_2N].

As shown in **Fig. 4** the calculated values of the [emim][Tf_2N] agree well with the experimental values reported in the literature.

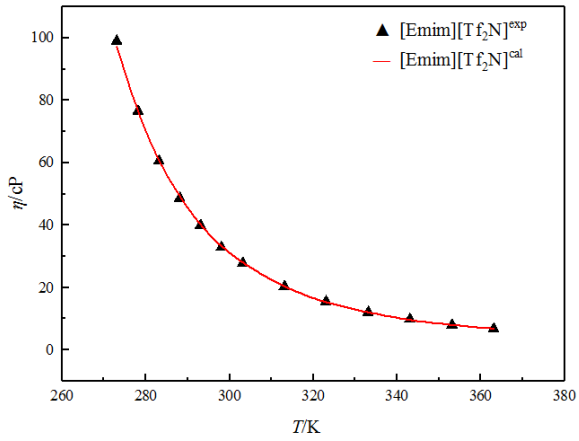

Fig. 4. Viscosity fitting effect of [emim][Tf_2N].

Fig.5 shows the calculated value of the saturated vapor pressure of [emim][Tf_2N] and the experimental values reported in the literature. It can be seen from **Fig. 5** that as the temperature increases, the agreement between the experimental value and the calculated value decreases. But the degree of agreement is high within a certain range.

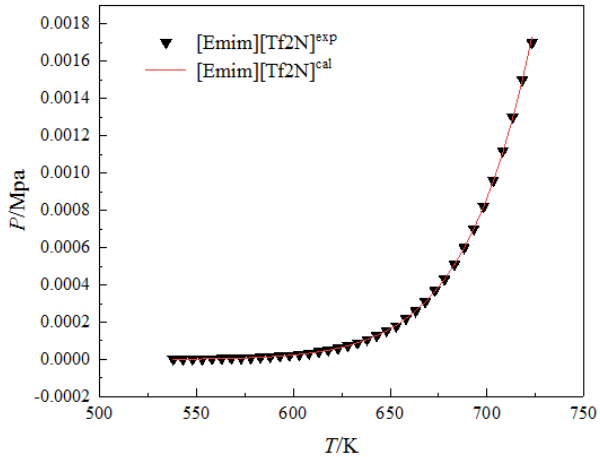

Fig. 5. Vapor pressure fitting effect of [emim][Tf2N] saturated .

Fig. 6 is a comparison of the calculated values of the thermal conductivity of the

[emim][Tf_2N] and the experimental values reported in the literature. Since the degree of thermal conduction with temperature is not significant and the data points are small, the range of the ordinate is small in the **Fig.6.** The image presented is deviated greatly.

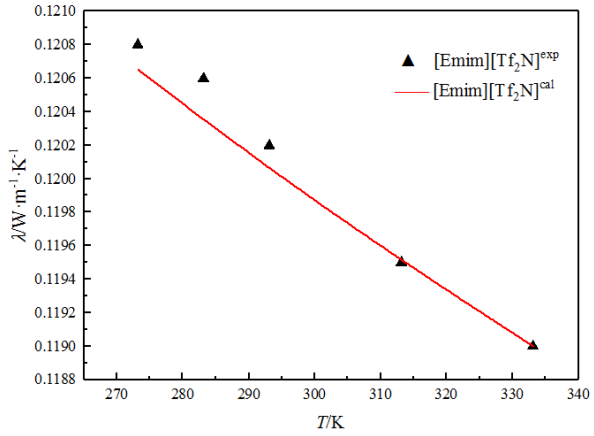

Fig. 6. Thermal conductivity fitting effect of [emim][Tf_2N].

As shown in **Fig.7** due to the data reported in the literature, there are many results with large differences between the temperatures, and the calculated values of the [emim][Tf_2N] surface tension parameters are in agreement with the experimental values.

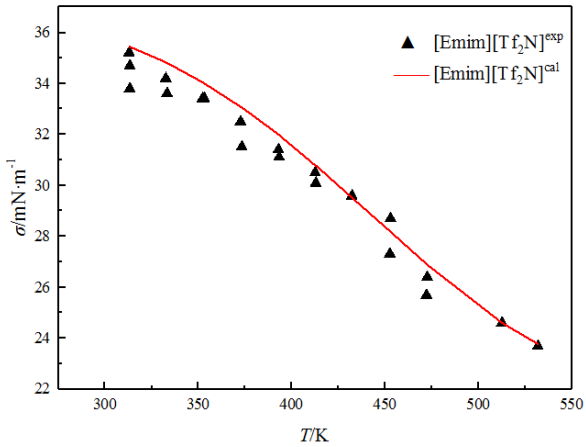

Fig. 7. Surface tension calculation formula fitting effect of [emim][Tf_2N].

4.2.Gases solubilities in the ILs.

By measuring the solubility of CO_2 in [emim][Tf_2N], CO_2 solubility data at different temperatures (303.15 K, 313.15 K, 323.15 K) and pressures from 0 to 0.6 MPa can be obtained. The specific results are shown in **Table 5.** The data in **Table 5** is plotted and the results are shown in **Fig. 8.**

Table 5. Solubility of CO_2 in [emim][Tf_2N] equilibrium pressure.

T=303.15 K		T=313.15 K		T=323.15 K	
P/MPa	10^3x	P/MPa	10^3x	P/MPa	10^3x
0.0971	21.25	0.0944	18.34	0.0926	14.04
0.2565	56.26	0.1889	36.26	0.2248	36.47
0.3115	68.78	0.2639	50.38	0.3436	55.13

0.3837	84.97	0.3255	63.35	0.4107	66.59
0.4524	98.26	0.4064	78.88	0.5063	80.03
0.5412	117.97	0.4500	86.83	0.5512	87.31

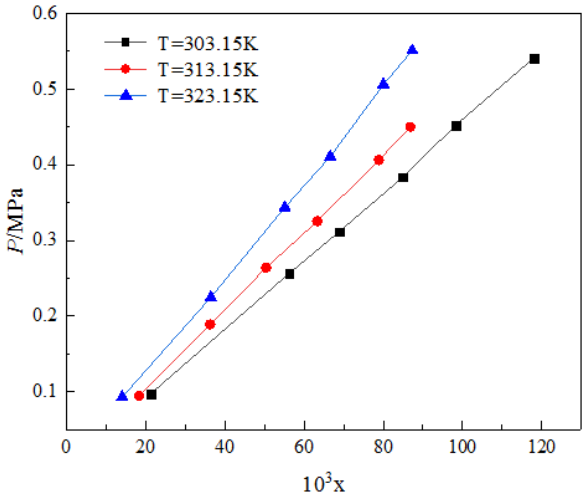

Fig.8. Solubility of CO_2 in [emim][Tf_2N].

5.Development of a conceptual process

The chemical process simulation and evaluation is the basis of new process development. This chapter mainly simulates the [emim][Tf_2N] capture CO_2 process, and carries out process optimization research.

The conceptual process employs each of the two ILs as physical solvents to selectively capture CO_2 from a fuel gas stream, which was generated from the Shenhua Guohua Jinjie subcritical coal-fired unit and shifted to a pressure and a temperature of 0.1 Mpa and 323.15 K, respectively. The composition of this shifted gas is given in **Table 6**. For a 600 MW power plant the flow rate of the fuel gas stream is 85000 $Nm^3.h^{-1}$.

Table 6. Flue gas composition.

Composition	mol %
N_2	79
CO_2	15
O_2	5
H_2O	1

The process flow of ionic liquid capture CO_2 is shown in **Fig.9**. The ionic liquid capture CO_2 process mainly includes the following operation units:

（1）Flue gas pretreatment unit

The flue gas discharged from the coal-fired power plant is desulfurized and washed, and the temperature is lowered to323.15 K. First, it is compressed to the absorption operating pressure by the multi-stage compressor unit (MC-1). After each stage of the compressor, a cooler is installed to compress The machine is cooled down and the condensate in the gas is removed. After multi-stage compression, enter the dryer (DRY-1) and further dry;

（2）Absorption unit

The pretreated gas enters from the bottom of the absorption tower (AB-1) and is in

countercurrent contact with the ionic liquids. The CO_2 is absorbed by the ionic liquids, and the unabsorbed gas is discharged from the top of the tower;

（3）Solvent desorption unit

The ionic liquid with a large amount of CO_2 discharged from the bottom of the absorption tower is called a rich liquid, and the rich liquid enters the first-stage flash tank (FL-1), and the gas such as N_2 and O_2 is released by reducing the pressure to improve the purity of the final product. The released N_2, O_2 and part of CO_2 are compressed by a recycle compressor (CMP-1), cooled by a cooler (HX-2) and then circulated to an absorption tower (ABS-1). The purified rich liquid enters the secondary flash tank (FL-2) and desorbs under reduced pressure to obtain the product CO_2. The desorbed ionic liquid is called the lean liquid, and the lean liquid passes through the circulation cooler (HX-1) and the circulation pump (P-1) Return to the absorption tower for cyclic absorption.

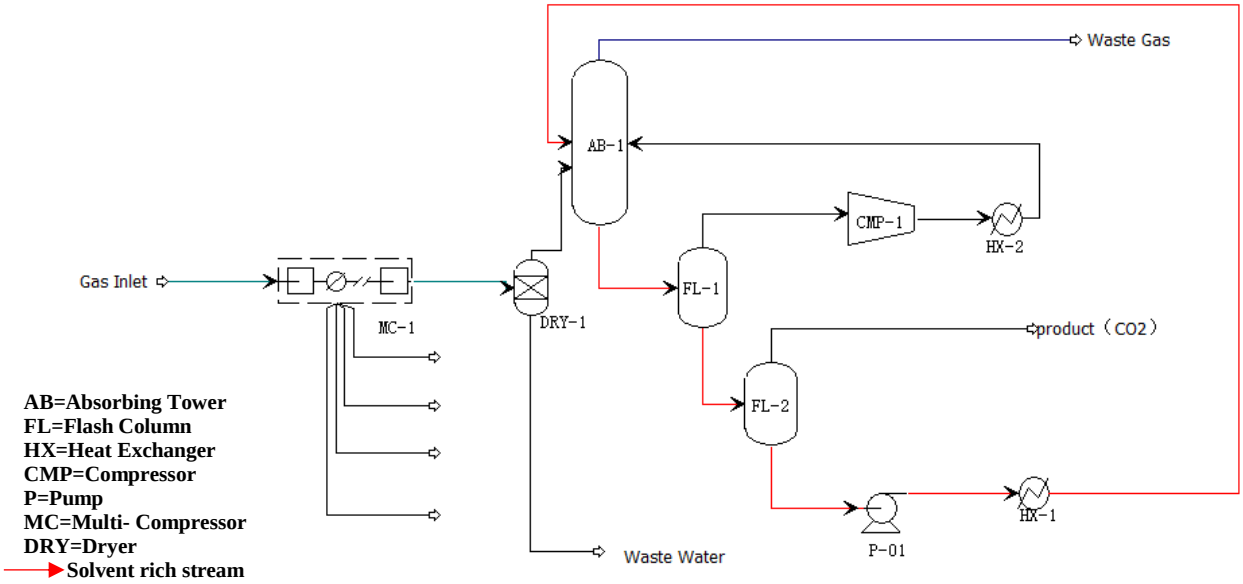

Fig.9. Process flow diagram for CO_2 capture using [emim][Tf2N].

The main equipments for the process simulation are absorption tower (AB-1), first-stage flash tank (FL-1), secondary flash tank (FL-2) and circulation pump (P-01). The parameter settings are shown in **Table 7**.

Table 7. Key parameters for the CO_2 capture of main equipment.

Description	Unit
Absorption tower	
No. stages	30
Condenser	None
Reboiler	None
Pressure drop	0.01 /Mpa
IL-IN feeding position	On stage 1
10 feeding position	On stage 30
Primary flash tank / heat load	0 / kW
Multi-stage compressor unit	
Compressor stage	5

Interstage cooler temperature	323.15K
Types	Mcompr(Isentropic)
Secondary flash tank / heat load	0 / kW
Circulation pump / efficiency	75%

6. Results and discussion

6.1 The effect of the physical properties of ionic liquids on the process

The ionic liquids have good designability, and can design ionic liquids with corresponding functions and properties according to requirements. Physical properties such as density, constant pressure heat capacity, surface tension, thermal conductivity, and viscosity are important properties of ionic liquids. This paper intends to investigate the effects of the properties of ionic liquids on the capture process and heat exchanger selection based on the whole process simulation, thus providing key information for the screening and design of ionic liquids.

6.1.1 Density

The effect of the density of the ionic liquids on the carbon capture process was investigated. **Fig.10** shows the effect of the density of the ionic liquid on the solvent circulation and unit energy consumption when capturing unit CO_2. It should be noted that the absorption pressure is the same and the multi-stage compressor energy consumption accounts for a large proportion. The unit energy consumption does not include the energy consumption of multi-stage compressors. As can be seen from the **Fig.10**, the density of the solvent is 0.5X, 1X and 2X, and the circulating solvent amount of 1 t CO_2 is 127.6 m^3, 49.6 m^3 and 24.9 m^3. Whenever the density doubles, the solvent is decreased by 61.1% and 49.8%, respectively. When the absorption capacity of the molar ionic liquids is the same, the larger the density, the smaller the volume of the ionic liquids, the smaller the circulation amount of the solvent, and the lower the energy consumption.

The effect of the density of the [emim][Tf_2N] on the volume distribution of the liquid phase in the absorption tower is shown in **Fig.11**. The higher the density, the smaller the liquid phase volume and the smaller the equipment required.

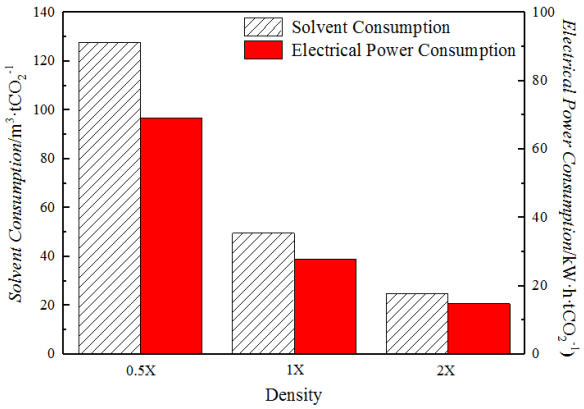

Fig. 10. Effect of [emim][Tf_2N] density on solvent circulation and energy consumption.

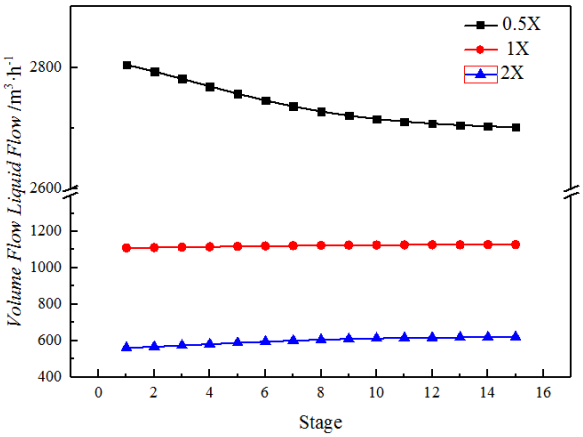

Fig. 11. The influence of the density of [emim][Tf_2N] on the volume distribution of liquid phase in absorber.

6.1.2 Constant pressure heat capacity

The effect of constant pressure heat capacity of ionic liquids on carbon capture process was investigated. When the ionic liquids absorbs CO_2, the heat is released, which causes the temperature of the solution in the tower to rise. The influence of the constant pressure heat capacity of the ionic liquid on the temperature distribution of the absorption tower is shown in **Fig.12**. The greater the constant pressure heat capacity, the smoother the temperature distribution curve in the absorption tower. A constant pressure ionic liquid with a large heat capacity can absorb more heat when the temperature rises by 1K. **Fig.13** further demonstrates that for every doubling of the constant pressure heat capacity, the solvent circulation is reduced by 3.7% and 2.0%, respectively. When the constant pressure heat capacity is small, the heat released by CO_2 will cause the temperature to rise sharply. The temperature rise will inhibit the further dissolution of CO_2. More ionic liquid is needed to achieve the same absorption effect. It causes an increase in the circulation of ionic liquids, which in turn requires more energy to capture unit CO_2.

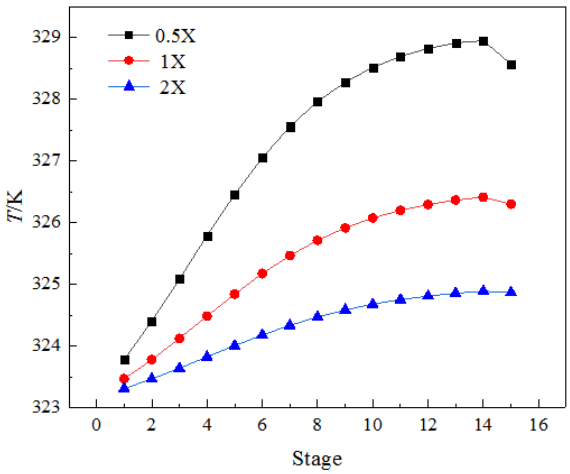

Fig.12. Influence of constant pressure heat capacity of [emim][Tf_2N] on temperature distribution curve of absorber

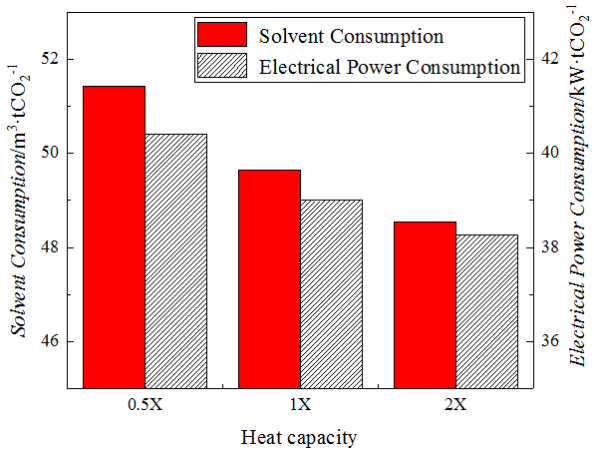

Fig. 13. The influence of the constant pressure heat capacity of [emim][Tf_2N] on the volume of solvent circulation and the energy consumption.

6.1.3 Surface tension, thermal conductivity, viscosity

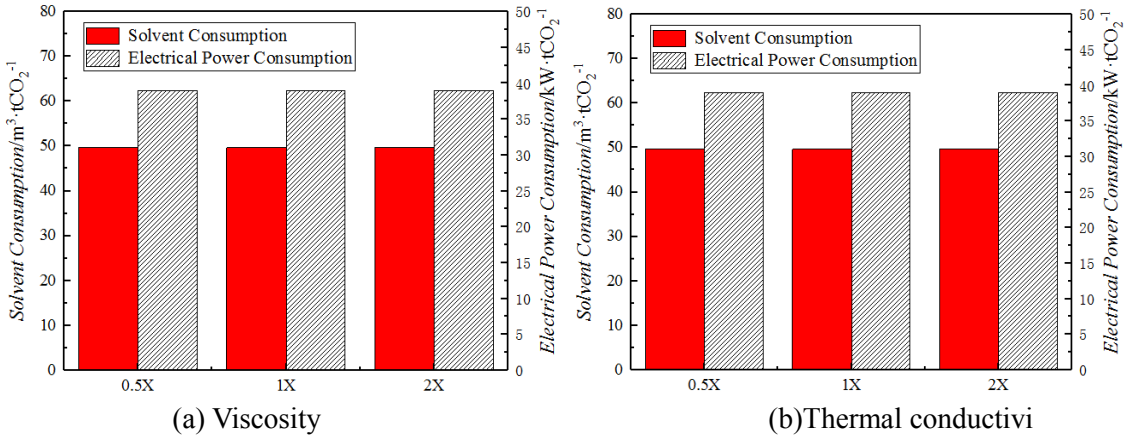

(a) Viscosity (b)Thermal conductivi

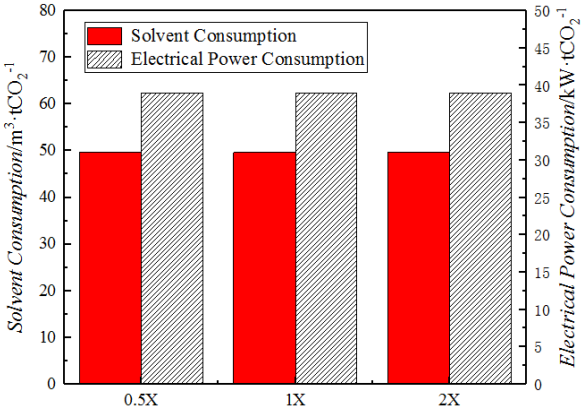

(c)Surface tension

Fig. 14. Effect of [emim][Tf_2N] physical properties on process energy consumption and [emim][Tf_2N] circulation

The whole process simulation mainly carries out material balance and energy balance calculation on the process. The viscosity, surface tension and thermal conductivity are not substituted in the material balance and energy balance calculation. Therefore, it is impossible to change the energy consumption and ionic liquids of the process by changing these factors. **Fig. 14** shows the effect of ionic liquids physical properties on the energy consumption of the process and the amount of ionic liquids circulation.

6.2 Process optimization

6.2.1 Process optimization

The temperature and liquid molar flow rate distribution in the absorption tower of the ionic liquids capture CO_2 process are shown in **Fig.10.** It can be seen from **Fig.15** that the temperature distribution in the absorption tower first rises and then decreases, and the temperature rise from the first tray to the eighth tray is larger . Because CO_2 is in contact with fresh ionic liquids, and a large amount CO_2 is absorbed by the ionic liquids with releasing a lot of heat. After the eighth block, the temperature rise rate is slowed down, the CO_2 dissolution tends to be balanced, and the temperature rise of the ionic liquid suppresses the absorption process.

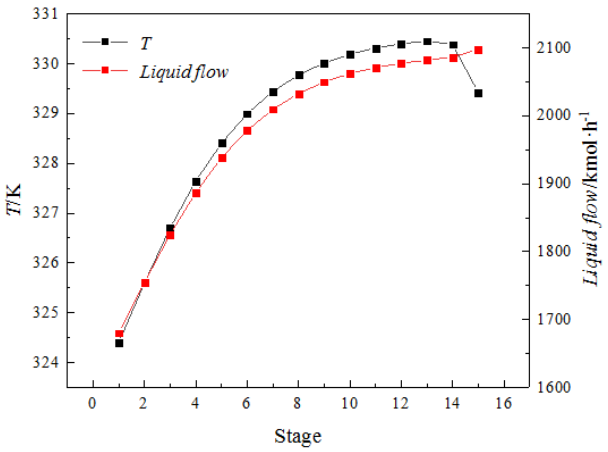

Fig.15. Temperature and liquid flow rate profiles of absorbers.

According to the above analysis, the inter-stage cooling is set between the 8th and 9th trays. A part of the solution is taken on the 8th tray and cooled to 313.15K through the heat exchanger (HX-3). Then the solution is fed in the 9th block. The optimized ionic liquids capture CO_2 process flow is shown in **Fig.16**. The process of dissolving CO_2 in the ionic liquids releases a large amount of heat. The reaction heat is removed by an intercooler (HX-3) which is disposed in the middle of the absorption tower to promote the dissolution of CO_2. Thereby the circulation amount of the ionic liquids were reduced.

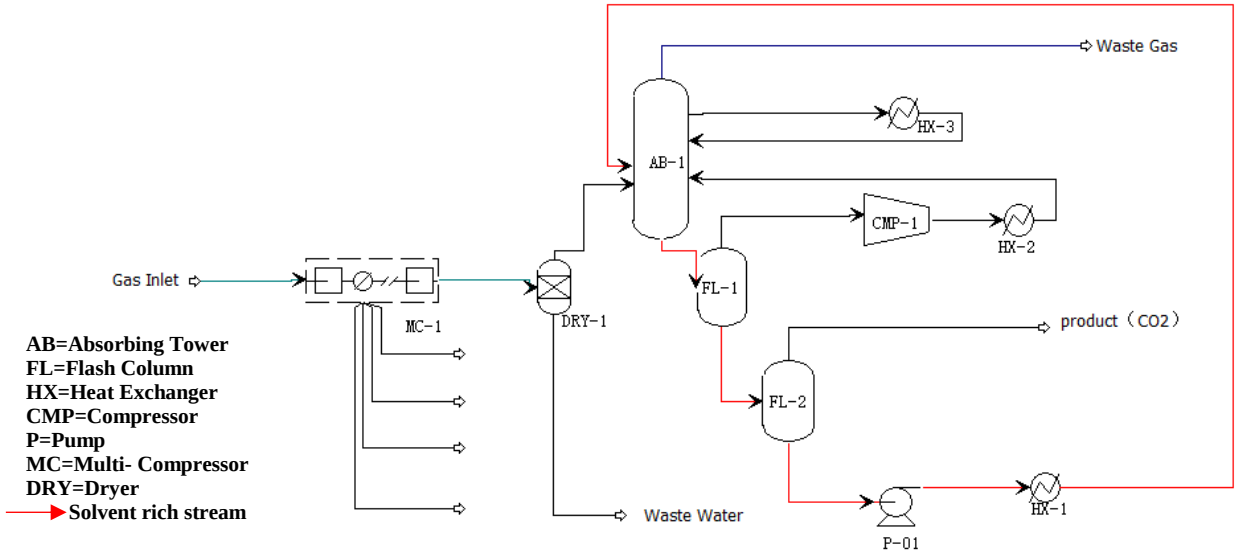

Fig.16. Modified process flow diagram for CO_2 capture using [emim][Tf_2N]

After optimization, the temperature distribution curve in the absorption tower is shown in **Fig.17**, which increases the inter-stage cooling and improves the temperature distribution in the absorption tower. **Table 8** shows the material balance results after process optimization.

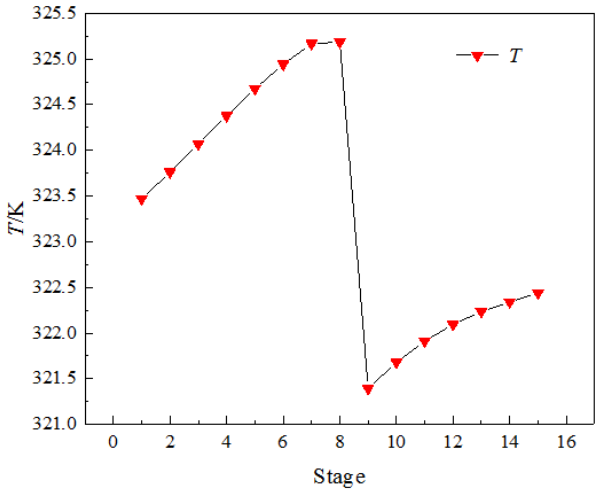

Fig.17. Modified temperature profiles of absorbers.

Table 8. Optimal simulation results of process.

		FLUGAS	GAS-01	RICH-1	CO_2
Phase		Vapor	Vapor	Liquid	Vapor
Temperature	K	323.15	323.46857	322.43714	319.67533
Pressure	Mpa	0.1	1.9	1.91	0.01
Molar Enthalpy	$Kcal.mol^{-1}$	-14.4957	-0.98367	-34.6778	-93.7808
Mass Enthalpy	$Kcal.kg^{-1}$	-475.0786	-34.5862	-99.3151	-2131.02
Molar Entropy	$Cal.mol^{-K}$	1.92883	-4.7394	-19.8089	5.918027
Mass Entropy	$Cal.gm^{-K}$	0.063215	-0.16664	-0.05673	0.134478
Molar Density	$Kmol.cum^{-1}$	0.037244	0.70927	4.282214	0.003764
Mass Density	$Kg.cum^{-1}$	1.136397	20.17241	1495.219	0.165639
Enthalpy Flow	Gcal/hr	-54.35887	-3.13638	-158.075	-47.5194
Average MW		30.512212	28.4411	349.1695	44.00748
Mole Flows	Kmol.hr-1	3750	3188.445	4558.389	506.7076
CO_2	Kmol.hr-1	562.5	38.52342	550.0002	506.6324
H_2O	Kmol.hr-1	37.5	0	0	0
N_2	Kmol.hr-1	2962.5	2962.429	2.798901	0.067879
[emim][Tf_2N]	Kmol.hr-1	0	3.70E-11	4005.358	2.98E-10
O_2	Kmol.hr-1	187.5	187.4923	0.230962	0.007296
Mole Fractions					
CO_2		0.15	0.012082	0.120657	0.999852
H_2O		0.01	0	0	0
N_2		0.79	0.929114	0.000614	0.000134
[emim][Tf_2N]		0	1.16E-14	0.878679	5.88E-13
O_2		0.05	0.058804	5.07E-05	1.44E-05
Mass Flows	$Kg.hr^{-1}$	114420.8	90682.88	1591650	22298.93
Volume Flow	$Cum.hr^{-1}$	100687.34	4495.391	1064.493	134623.3

6.2.2Heat exchanger design

Heat exchangers are common equipment in chemical processes. The physical properties of ionic liquids in carbon capture processes may have an impact on the design and selection of heat exchangers. Therefore, this section will treat the density, viscosity and thermal conductivity of ionic liquids. Physical properties such as coefficient and constant pressure heat capacity were investigated. Requirements: 5000 $mol.h^{-1}$ of ionic liquids (some properties

are different from [emim][Tf_2N], the rest of the properties are the same) from 328.15 K to 323.15 K, using circulating cooling water (305.15K→ 313.15K) for cooling, The effects of various physical properties on heat transfer area and average heat transfer coefficient were investigated.

As can be seen from **Fig.18-21**,the greater the density and thermal conductivity of the ionic liquids, the smaller the heat exchange area required to accomplish the same heat transfer requirements. The greater the viscosity of the ionic liquids, the smaller the heat exchange area required to accomplish the same heat transfer requirements. The larger the constant pressure heat capacity of the ionic liquids, the more the unit mass ionic liquids drops by 1 K, so that the heat transfer coefficient is larger. Therefore, in the future, it is possible to find an ionic liquids having a large density, a thermal conductivity, and a constant heat capacity, and a small viscosity as an absorbent

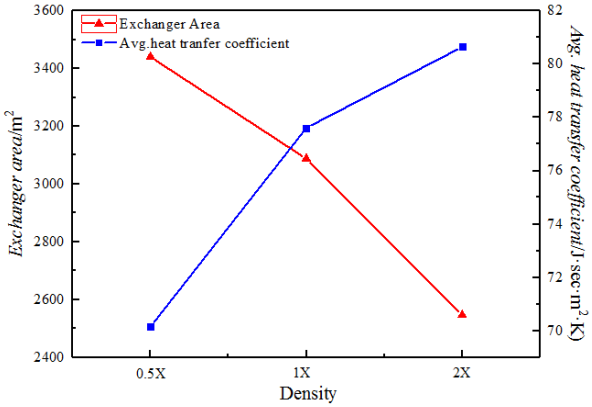

Fig.18. Effect of density of ionic liquid on heatexchanger area and average heat transfer coefficient of heat exchanger

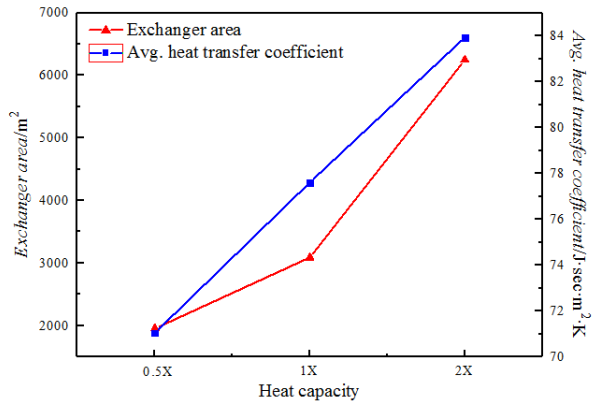

Fig.19. Effect of constant pressure heat capacity of ionic liquid on heat transfer area and average heat transfer coefficient of heat exchanger.

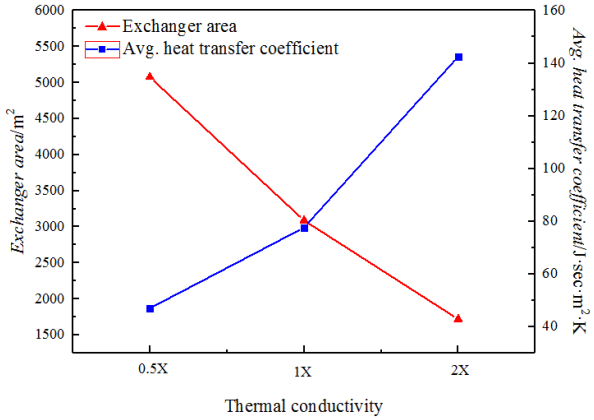

Fig.20. Effect of thermal conductivity of ionic liquid on heat exchanger area and average heat transfer coefficient of heat exchanger

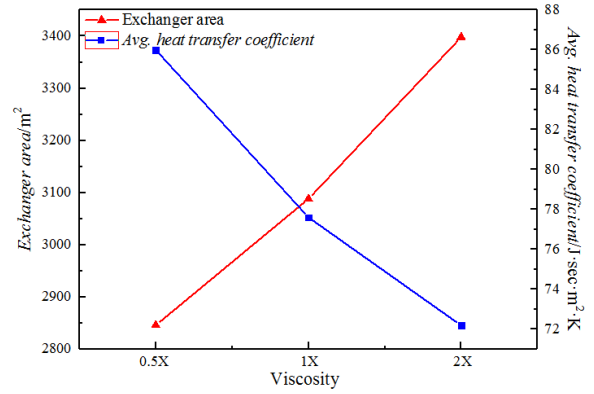

Fig.21. Effect of viscosity of ionic liquid on heatexchanger area and average heat transfer coef ficient of heat exchanger

6.3 Energy analysis

Under the premise of meeting the following design requirements: CO_2 capture rate is 90%, CO_2 mass purity is higher than 99.5%, and the process simulation results, key parameters, materials and energy consumption before and after optimization are compared. The specific results are shown in **Table 9**. It can be seen from **Table 9** that the optimized lean liquid circulation and power consumption are significantly reduced, and the rich liquid load is increased. However, due to the addition of a cooler, the consumption of cold utility projects has increased.

Table 9 . Simulation results and key parameters for process.

	Before optimization	Optimized
Lean liquid circulation /kmol.h^{-1}.t^{-1}CO_2	191.1	180.7
CO_2 lean liquid load	0.0054	0.0058
CO_2 rich liquid loading	0.130	0.137
Power consumption /kWh·t^{-1}CO_2	604.2	602.6
Cold utility consumption /GJ·t^{-1}CO_2	-2.22	-2.53

Compared with the traditional alcohol amine solution trapping process, the ionic liquid trapping CO_2 process proposed in this chapter consumes much different forms of energy. The traditional process consumes mainly heat energy, while the ionic liquid absorbs the process.

Mainly electric energy. The traditional MEA regeneration energy consumption is 3.59~3.7 $GJ \cdot t^{-1}CO_2$ [17, 18]. The power consumption of each operating unit is given in **Table 10**. As can be seen from **Table 10**, the power consumption requirement of the system is 13.437 MW. The consumption of compression of the flue gas accounts for about 93.8% of the total power consumption. Before each optimization, 1 ton of CO_2 is consumed to consume 2.175 GJ of electric energy, and after optimization, 2.169 GJ is needed, and the energy consumption is much lower than that of the conventional process.

Table 10. Power requirement of the conceptual process.

Bit number	Equipments	Consumption /MW
MC-01	Multi-stage compressor	12.613
C-01	Compressor	0.053
P-01	Circulating pump	0.771
Total power consumption		13.437

7. Conclusions

In this paper, the Aspen simulation and evaluation of [emim][Tf_2N] capture CO_2 in flue gas from coal-fired power plants was developed. The process simulation and optimization results show that The traditional MEA regeneration energy consumption is 3.59~3.7 GJ/t CO_2. Only 2.169 GJ is needed for each ton of CO_2 after optimization, which is superior to the traditional process. This indicates that [emim][Tf_2N] can be used as an excellent absorbent for CO_2.

The effect of the ionic liquid's own properties on process energy consumption and solvent circulation was discussed. The results show that compared with the reference [emim][Tf_2N], the ionic liquids with a density of 0.5 times the reference increased the solvent circulation and energy consumption by 61.1% and 59.7%, respectively. The circulating and energy consumption of the liquid solvent were reduced by 49.8% and 46.7% when density is twice the reference ionic liquids. The constant pressure heat capacity was 0.5 times that of the reference ionic liquid, and the solvent circulation and energy consumption were increased by 3.7% and 3.5%, respectively. The constant pressure heat capacity was twice the ionic liquids of the reference material, and the solvent circulation amount and energy consumption were reduced by 2.0% and 2.1%, respectively.

This study provides an important data foundation for related research. The CO_2 capture process designed and developed with ionic liquids as absorbents has a good application prospect. The simulation and evaluation results will provide guidance for engineering applications and ionic liquids design.

Acknowledgments

This work was financially supported by the Zhejiang Provincial Natural Science Foundation of China（LY16B060014），State Key Laboratory of Chemical Engineering （No. SKL-ChE-08A01）and the Innovation and Development of Marine Economy Demonstration.

Nomenclature

C_{pi} Molar heat capacity of liquid， $J \cdot mol^{-1} \cdot K^{-1}$

ρ_i Liquid density,$g.cm^{-3}$

M_i Molecular weight,$g.mol^{-1}$

N Number of group appearances in molecule

P System pressure, Mpa

P_b Standard atmospheric pressure, 0.101325 Mpa

P_c Critical pressure, Mpa

p_i^s Saturated vapor pressure ,Mpa

R Universal gas constant ,8.314 $J \cdot mol^{-1} \cdot K^{-1}$

T_b Boiling point temperature,K

T_c Critical temperature,K

V Molar volume, $cm^3.mol^{-1}$

x Solubility, mole of gas per total number of mole

x_i Liquid phase mole fraction

y_i Gas phase mole fraction

Z Compression factor

Z_c Critical compressibility

$Z_i^{*,RA}$ Rackett equation parameters

η_i Liquid viscosity,mPa•s

σ_i Liquid surface tension,$mN \cdot m^{-1}$

γ_i Activity coefficient

γ_i^{∞} Infinite dilution activity coefficient

φ_i^V Gas phase fugacity coefficient

λ_i Thermal Conductivity， $W \cdot m^{-1} \cdot K^{-1}$

ΔT_b Normal boiling temperature contribution,K

ΔP_c Critical pressure contribution, Mpa

ΔT_c Critical temperature contribution,K

ΔV_c Critical volume contribution,$cm^3.mol^{-1}$

Δ_{ij} NRTL binary interaction parameter

References

[1] P. Maas, N. Nauels , L. Zhao , P. Markewitz , V. Scherer , M. Modigell , D. Stolten , J.-F. Hake. Energetic and economic evaluation of membrane-based carbon capture routes for power plant processes. *Int J Greenh Gas Con*. 44 (2016) 124–139

[2] K.A. Mumford, Y.Wu, K.H. Smith, G.W. Stevens. Review of solvent based carbon-dioxide capture technologies. *Front. Chem. Sci. Eng* .9（2015）125–141

[3] Shupanxiang Chen, Xiaoming Han, Xiaoyu Sun, Xiao Luo, Zhiwu Liang. The comparative kinetics study of CO_2 absorption into non-aqueous DEEA/MEA and

DMEA/MEA blended systems solution by using stopped-flow technique. *Chem.Eng.J.* https://doi.org/10.1016/j.cej.2019.03.171

[4] Ke-Jun Wu, Qiao-Li Chen, Chao-Hong He, Speed of sound of ionic liquids: Database, estimation, and its application for thermal conductivity prediction. *AIChE. J*. 60(2014) 1120–1131.

[5] K.R.Seddon, Ionic Liquids for Clean Technology. *J .Chem.Technol.Biot*. 68(4) (2010)351-356.

[6] X.P. Zhang, X.C. Zhang, H.F. Dong, Z.J. Zhao, S.J. Zhang, Y. Huang .Carbon capture with ionic liquids: overview and progress. *Energy. Environ. Sci.* 5 (2012)6668−6681.

[7] X. Liu, X. Zhang, G. Zhou, X. Yao, S.Zhang. All-atom and united-atom simulations of guanidinium-based ionic liquids. *Sci. China. Chem.* 55(2012) 1573−1579.

[8] M. P. Gimeno, M. C. Mayoral, J. M. Andres. Influence of temperature on CO_2 absorption rate and capacity in ionic liquids. Energ Fuel. 27(2013)3928−3935.

[9] S.J. Zhang, X.P.Zhang, Y.S.Zhao, G.Y. Zhao, X.Q.Yao, H.W.Yao. A novel ionic liquids-based scrubbing process for efficient CO_2 capture. *Sci. China.Chem*.53(2010)1549−1553.

[10]S.J. Zhang, X.L. Yuan, Y.H. Chen, X.P. Zhang. Solubilities of CO_2 in 1-butyl-3-methylimidazolium hexafluorophosphate and 1,1,3,3-Tetramethylgu anidium lactate at elevated pressures. *J. Chem. Eng*. 50(2005)1582−1585.

[11] S. J. hang, Y. H. Chen, R. X. F.Ren, Y. Q .Zhang, J. M. Zhang, X. P. Zhan. Solubility of CO_2 in sulfonate ionic liquids at high pressure. *J. Chem. Eng.* 50(2005) 230−233

[12] J.F. Brennecke, B.E. Gurkan. Ionic liquids for CO_2 capture and emission reduction. *J . Phys. Chem. Lett.* 24(2010)3459-3464.

[13] Mahinder Ramdin，Theo W. de Loos，Thijs J. H. Vlugt. State-of-the-art of CO_2 capture with ionic liquids. *Ind .Eng .Chem .Res* . 51(2012)8149-81

[14] Dan H. Blanchard, E.J. Beckman,J.F. Brennecke. Green processing using ionic liquids and CO_2. *Nature*.399(1999)28-29.

[15] S Zeng, X Zhang, L Bai, X Zhang, H Wang. Ionic-Liquid-Based CO_2 Capture Systems: Structure, Interaction and Process. *Chem. Rev.* 117(2017) 9625.

[16] M .B. Shiflett, D.W. Drew, R.A. Cantini, A Yokozeki. Carbon Dioxide Capture Using Ionic Liquid 1-Butyl-3-Methylimidazolium Acetate, *Energ .Fuel*. 24(2010) 5781-5789

[17] T.Ma, J Wang, Z Du, Z Du, A. A. Abdeltawab, A.M. Al-Eniz, X Chen, G Yu. A process simulation study of CO_2, capture by ionic liquids. *Int. J. Greenh Gas Con.* 58 (2017)223-231.

[18] Y.Huang, X.Zhang, X.Zhang, H.Dong, S.Zhang. Thermodynamic Modeling and Assessment of Ionic Liquid-Based CO_2 Capture Processes, *Ind .Eng .Chem .Res* . 53(2014)11805-11817.

[19] O.M. Basha, M.J. Keller, D.R. Luebke, K.P. Resnik, B.I. Morsi. Development of a conceptual process for selective CO_2 capture from fuel gas streams using [hmim][Tf_2N] ionic liquid as a physical solvent. *Energ .Fuel*. 27(2013) 3905-3917.

[20] O.M. Basha, Y.J. Heintz, M.J. Keller, D.R. Luebke, K.P. Resnik, B.I. Morsi. Development of a conceptual process for selective capture of CO_2 from fuel gas streams using two TEGO ionic liquids as physical solvents. *Ind .Eng .Chem .Res* . 53(2014) 3184-3195.

[21] A.Yokozeki, M.B. Shiflett. Hydrogen purification using room-temperature ionic liquids. *Appl. Energ.* 84(2007)351-361.

[22] M.B. Shiflett, A.Yokozeki. Solubility of CO_2 in room temperature ionic liquid [hmim][Tf2N]. *J . Phys. Chem. B.* 111(2007) 2070-2074

[23] A.M. Schilderman, S Raeissi, C.J. Peters. Solubility of carbon dioxide in the ionic liquid 1-ethyl-3-methylimidazolium bis(trifluoromethylsulfonyl)imide. *Fluid. Phase. Equilib.* 260(2007) 19-22.

[24] A.F. Ferreira, P.N. Simões, A.G.M. Ferreira. Quaternary phosphonium-based ionic liquids: Thermal stability and heat capacity of the liquid phase. *J.Chem.Thermodyn.* 45(2012) 16-27.

[25] F.Heym, W.Korth, B.J.M. Etzold, C.Kern, A.Jess. Determination of vapor pressure and thermal decomposition using thermogravimetrical analysis. *Thermochim Acta*. 622(2015)9-17.

[26] A.P. Fröba, M.H. Rausch, K.Krzeminski, D.Assenbaum, P.Wasserscheid. Thermal Conductivity of Ionic Liquids: Measurement and Prediction. *Int. J. Thermophys.* 31(2010) 2059-2077.

[27] M.Tariq, A.P. Serro, J.L. Mata, B.Saramago, J.Esperança, J.N.C. Lopes, L.P.N. Rebelo. High-temperature surface tension and density measurements of 1-alkyl-3-methylimidazolium bistriflamide ionic liquids. *Fluid .Phase. Equilibr.* 294(2019) 131-138.

[28] V.M. Mecea. Is quartz crystal microbalance really a mass sensor. *Sensor. Actuat. A-Phys.* 128(2006)270-277.

[29] Z.Lei, H.Inomata, H.Ohyabu, Y.Sato, R.L. Smith. Solubility, swelling degree and crystallinity of carbon dioxide–polypropylene system.. *J. Supercrit. Fluid.* 40(2007) 452-461.

[30] Z.Lei, J.Yuan, J Zhu. Solubility of CO_2 in Propanone, 1-Ethyl-3-methyl- imidazolium Tetrafluoroborate, and Their Mixtures. *J. Cheml. Eng. Data.* 57(2010) 3458–3466.

[31] E.K. Shin, B.C. Lee. High-Pressure Phase Behavior of Carbon Dioxide with Ionic Liquids: 1-Alkyl-3-methylimidazolium Trifluoromethanesulfonate. *J. Cheml. Eng. Data*. 53(2008) 2728-2734.

[32] J.Zhang, Q.Zhang, Qiao.A. Botao, Y.Deng. Solubilities of the Gaseous and Liquid Solutes and Their Thermodynamics of Solubilization in the Novel Room-Temperature Ionic Liquids at Infinite Dilution by Gas Chromatography. *J. Cheml. Eng. Data*. 52(2007) 2277-2283.

[33]Yan Fei Chen. Experment Study and Quantum Chemistry Simulation on the Absorption of CO_2 in Ionic Liquid. M.S .Thesis, ZheJIiang Univ Technol,China,2014(in chinese).

[34] L.P. Rebelo, J.N. Canongia Lopes, J.M.Esperança , E Filipe. On the critical temperature, normal boiling point, and vapor pressure of ionic liquids. *J . Phys. Chem. B.* 109(2005): 6040-6043.

[35]J.O.Valderrama,R.E.Rojas.Critical Properties of Ionic Liquids Revisited.*Ind .Eng .Chem .Res.* 48(2009) 6890-6900.

[36] T.Makino, M.Kanakubo, Y.Masuda, T.Umecky, A.Suzuki. CO_2 absorption properties, densities, viscosities, and electrical conductivities of ethyl- imidazolium and 1-ethyl-3-methylimidazolium ionic liquids. *Fluid .Phase. Equilib.* 362(2014) 300-306.